Nanoscale

Cleavable Energy Transfer Labeled Oligonucleotide Probe for Enhanced Isothermal Amplification Detection and Nano Digital Chip-based Readout

Journal:	*Nanoscale*
Manuscript ID	NR-ART-07-2024-003142.R1
Article Type:	Paper
Date Submitted by the Author:	05-Nov-2024
Complete List of Authors:	Liu, Li; University of California Riverside Dollery, Stephen; Biological Mimetics Inc Tobin, Gregory; Biological Mimetics Inc Lu, Guoyu; University of Georgia Du, Ke; University of California Riverside,

ARTICLE

Cleavable Energy Transfer Labeled Oligonucleotide Probe for Enhanced Isothermal Amplification Detection and Nano Digital Chip-based Readout

Received 00th January 20xx,
Accepted 00th January 20xx

DOI: 10.1039/x0xx00000x

Li Liu, [a] Stephen J. Dollery, [b] Gregory J. Tobin, [b] Guoyu Lu [c] and Ke Du *[a]

Quantitative analysis of human papillomavirus (HPV)-infected cervical cancer is essential for early diagnosis and timely treatment of cervical cancer. Here, we introduce a novel energy transfer-labeled oligonucleotide probe to enhance the loop-mediated isothermal amplification (LAMP) assay for highly sensitive and specific detection of HPV 16. Conducted as a single-step assay within a digital nanofluidic chip featuring numerous reaction reservoirs, our method facilitates target amplification under isothermal conditions. Targeting an HPV 16 gene, our chip demonstrates the capability to detect HPV DNA at concentrations as low as 1 fM, spanning a dynamic range of five orders of magnitude. Importantly, our nano digital chip allows for highly quantitative detection of target genes at low concentrations, with the correlation between target concentration and the number of microwells exhibiting fluorescence signals. Furthermore, we have developed a computer vision method for automated and 100% accurate quantification of target concentrations. This research holds promising applications in clinical diagnosis and is poised for seamless integration into both hospital and point-of-care settings.

Introduction

Cervical cancer is the fourth most common cancer in women globally, and in almost all instances this begins with Human papillomavirus (HPV) infection.[1] The two most common high-risk genotypes, HPV16 and 18, are responsible for over 70% of cervical cancer cases.[2] Due to their elevated sensitivity and specificity, HPV DNA tests have become the gold standard for cervical cancer diagnosis.[3] However, these PCR-based DNA tests rely on bulky and expensive instruments such as thermal cyclers, making them impractical for point-of-care (POC) settings.[4] In recent years, nucleic acid isothermal amplification detection has emerged as a promising alternative to traditional PCR due to its simplicity, speed, cost-effectiveness, and high sensitivity.[5] Various nucleic acid isothermal amplification methods have been developed, including loop-mediated isothermal amplification (LAMP),[6–8] recombinase polymerase amplification (RPA),[9–11] rolling circle amplification (RCA),[12–14] and nucleic acid sequence-based amplification (NASBA).[15,16] Even though highly promising, most isothermal amplification detection methods have limitations such as a lack of quantitative detection capabilities, occasional unexpected non-specific amplification signals, and relatively high background signals.[17]

Microfluidic platforms have revolutionized the field of molecule detection by offering a highly miniaturized, cost-effective, and efficient approach for handling fluids at the microscale and even the nanoscale. These platforms—including droplet-based microfluidics, paper-based microfluidics, electrokinetic microfluidics, surface plasmon resonance (SPR) microfluidics, and optofluidics—each offer unique advantages that make them suitable for a wide range of applications. For example, droplet-based microfluidic was high throughput, low reagent consumption and have excellent isolation of reactions.[18] Paper-based microfluidic device are particularly attractive as low-cost, portable and user-friendly platforms, ideal for point-of-care testing.[19] Electrokinetic microfluidics, on the other hand, excels in sensitivity and offers precise control over sample movement without relying on moving mechanical parts.[20] SPR microfluidic platforms leverage the interaction between light and a metallic surface, allowing real-time, label-free monitoring of biomolecular interactions with high sensitivity.[21] Similarly, optofluidic platforms combine optical and fluidic technologies, enabling particle manipulation via optical tweezers, thus facilitating high-sensitivity detection and control over individual particles.[22] These diverse microfluidic platforms not only enhance sensitivity and processing speed but also require minimal sample volumes, making them promising tools in the continuous evolution of molecular detection technologies.

LAMP is one of the most widely applied isothermal amplification technologies in pathogen diagnostics.[23] The advantages of the LAMP reaction include high sensitivity and the use of multiple primers, which have exceptionally high specificity because a set of four primers with six binding sites must hybridize correctly to their target sequence before DNA biosynthesis occurs.[24] The reaction temperature is around 63°C, which avoids undesirable pre-amplification at room temperature.[25] In addition, LAMP exhibits a strong tolerance to inhibitors. Traditional detection methods relying on intercalating dyes like EvaGreen or SYBR Green can directly detect amplified targets but can have

[a] Department of Chemical and Environmental Engineering, University of California, Riverside, CA, USA.
[b] Biological Mimetics, Inc., 124 Byte Drive, Frederick, MD, USA.
[c] Intelligent Vision and Sensing Lab, University of Georgia, Athens, GA, USA.
† Supplementary Information available: [details of any supplementary information available should be included here]. See DOI: 10.1039/x0xx00000x

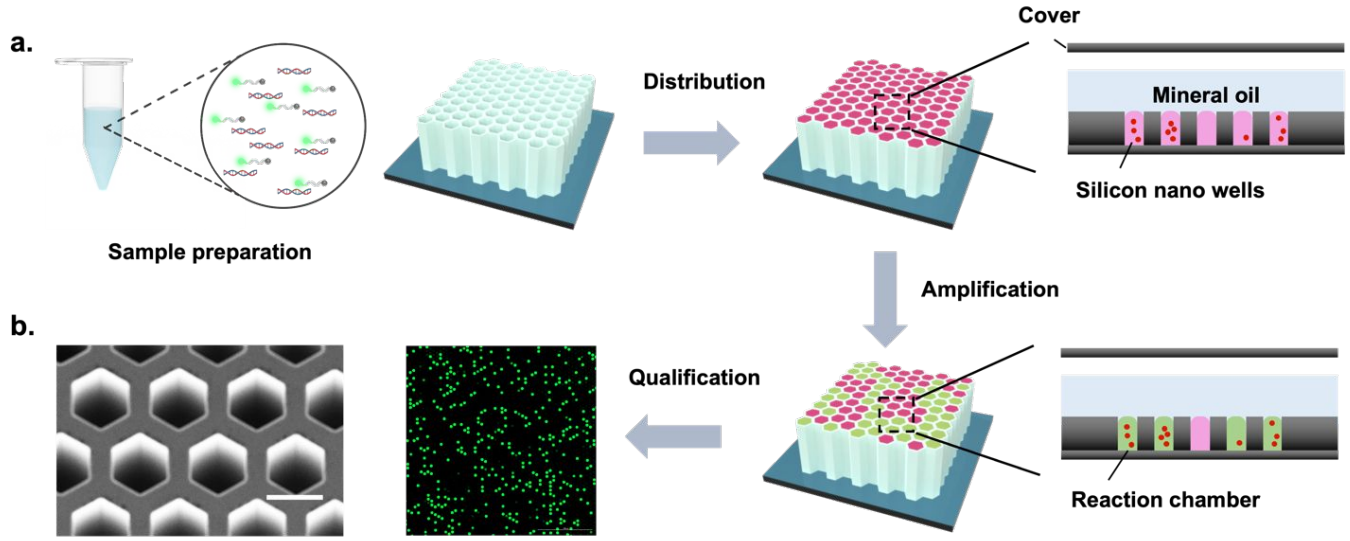

Figure 1 a. Schematic illustration of FQ LAMP assay. A one-pot reaction mixture is first prepared in one tube. The sample mixture is then distributed randomly into over ten thousand of microwells. When incubated at 63°C, each micro reaction with plasmid HPV 16 DNA target undergoes reaction and amplification, generating strong green fluorescence (positive spots), whereas not in those without target (negative spots). By detecting and counting the positive micro reactions (or spots), plasmid HPV 16 DNA can be quantified based on the proportion of positive spots. b. SEM image of micro digital chip. Scale bar is 60 μm.

drawbacks such as low selectivity and the potential inhibition of the amplification reaction,[26] thus requiring post-reaction analysis and causing false positives.[27] Recent progress in integrating LAMP with microfluidic platform has propelled point-of-care diagnostics by enabling compact, portable devices with enhanced efficiency, suitable for applications like for pathogen detection. For instance, Hao, et al developed a portable all-in-one device (PAD) for colorimetric detection of nucleic acids, capable of rapidly identifying various type of viral.[28] Cao, et al developed a LAMP-based microfluidic chip for both colorimetric and fluorescent readout for the simultaneous detection of multiple foodborne bacteria.[29] However, these methods lacked quantitative detection of nucleic acids. To address these issues, energy transfer-labeled oligonucleotide probes for sequence-specific fluorescence detection have been developed to improve the amplification process. Here, we introduce an innovative ribonuclease-dependent cleavable FQ LB (fluorophore–quencher Loop B) primer designed to augment the sensitivity and specificity of LAMP detection. This primer undergoes cleavage exclusively upon recognizing a specific nucleic acid sequence, thereby markedly enhancing detection specificity and minimizing background signals.

Digital micro-and nanofluidic detection chips have been developed in recent years with advantages over traditional methods, such as greater tolerance to inhibitory substances, higher sensitivity, and more accurate detection.[30] The combination of digital chips and nucleic acid amplification methods enables absolute quantification analysis of nucleic acid targets by distributing target molecules into small wells or droplets. When performing limited dilution into aliquots, those aliquots contain no target molecule or only one molecule. The target molecule concentration can then be derived by counting the number of positive aliquots. The isolation of aliquots eliminates the competition of primers and probes, which is especially important for detecting minute DNA targets.[31] Currently, there are two main strategies for generating isothermal reaction units, one of which involves using chamber microfluidic chips to generate reaction units. However, due to manufacturing process limitations, the number of chambers in microfluidic chips is limited as the chamber volume is relatively large, leading to a restricted dynamic range.[32] The other strategy involves using droplet microfluidic chips to generate monodisperse droplets. However, the process of droplet formation is relatively complex, and the stability of the droplets poses issues, making real-time reaction monitoring a significant challenge.[33]

In the work, we show a novel energy transfer-labeled oligonucleotide probe with improved fluorescence properties to create a highly sensitive and specific isothermal amplification of nucleic acids for sensitive and quantitative detection of HPV 16 sequences in plasmids that mimic dsDNA HPV genomes. The digital warm start assay is established through a LAMP-based reaction in sub-microliter aliquots within a digital nanofluidic chip. This reaction is a one-pot format FQ labeled primer isothermal amplification-based detection, preventing premature target amplifications at room temperature and enabling accurate digital quantification of nucleic acids. Further, separation of aliquots eliminates competition between primers and probes and largely reduces false positive signals. We apply machine learning algorithm to facilitate the straightforward derivation of quantitative relationships for target concentrations. Combining these advantages enables our system to be adapted in hospitals or POC settings for the quantification of sexually transmitted infections.

Results

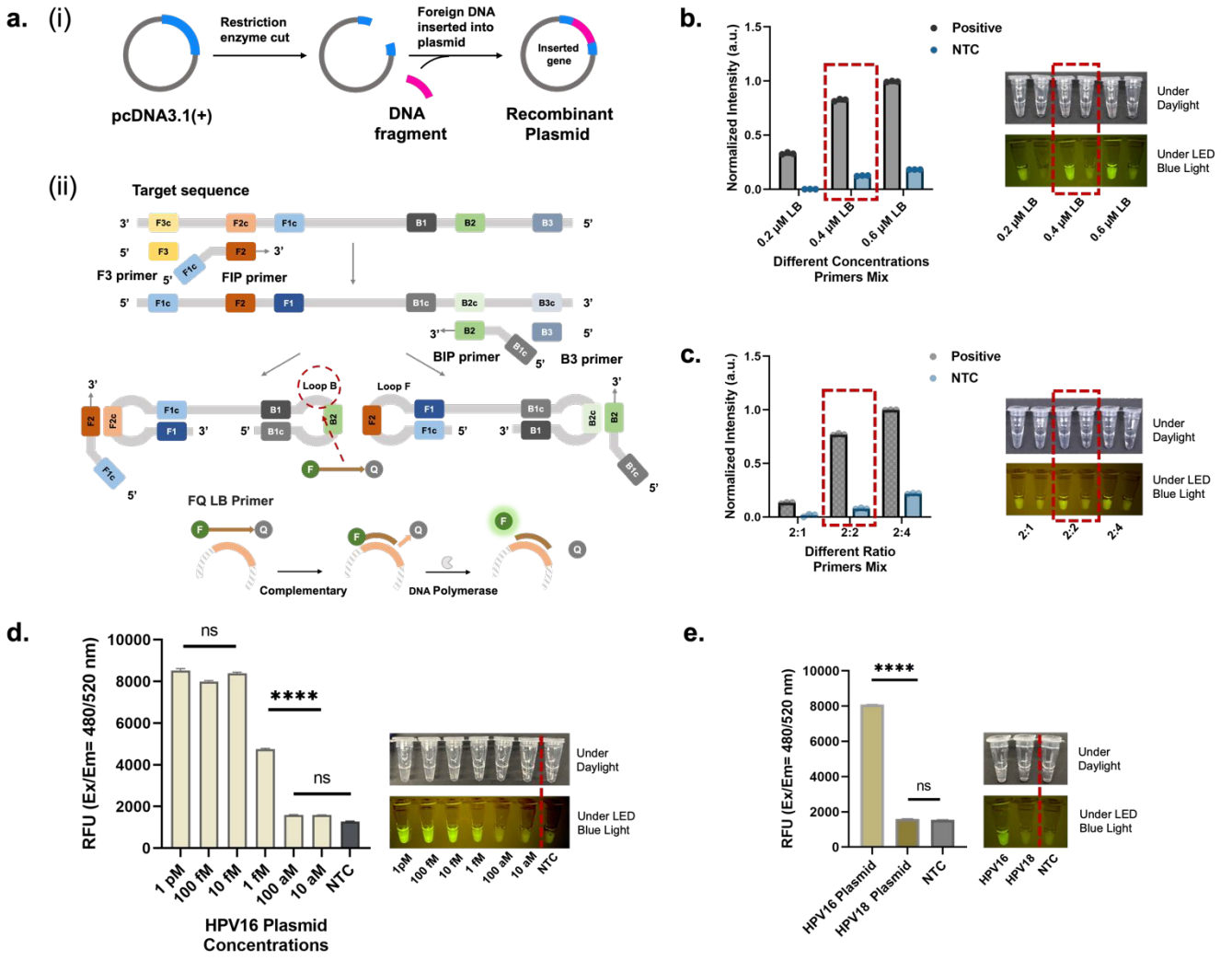

Figure 2. (a-i) HPV-L1 gene (450 bp) from HPV16 inserted into plasmid cDNA3.1(+) vector, making our target similar in size and sequence to HPV. (a-ii) Principle of the FQ-LAMP assay. In this assay, LAMP's loop backward (LB) primer was used to design the FQ LAMP probe. When the probe binds to the specific complementary target sequence, DNA polymerase degrades the probe, separating the fluorophore from the quencher, allowing the fluorophore to emit a signal that indicates the presence of the target sequence. b. The LAMP conditions were optimized for the reaction with a mixture of LB/FQ LB primers at concentrations of 0.2, 0.4, and 0.6 µM, respectively. c. The LAMP conditions were optimized for the reaction with a mixture ratio of LB/FQ LB primers were 2:1, 2:2, and 2:4, respectively. d. Endpoint fluorescence detection of the FQ LAMP after 45-min amplification of various concentrations of plasmid HPV 16 DNA targets, from 10 aM to 1 pM. e. Endpoint fluorescence detection of the Plasmid HPV 16 DNA target (1 pM) compared with plasmid HPV 18 DNA target (1 pM) and no template control. For each concentration's testing, error bars denote the standard deviation (n = 3). The asterisks represent statistical significance according to a t-test. *P ≤ 0.05, **P ≤ 0.01, ***P ≤ 0.001, ****P ≤ 0.0001.

The schematic of the digital nanofluidic chip based on the one-step LAMP assay is shown in Figure 1a. The primers were designed to amplify an HPV 16 L1 fragment gene sequence (GenBank accession MT316211.1). The FQ-LAMP reaction mixture was first prepared in an Eppendorf tube. The prepared reaction mixture was then distributed into a QuantStudio 3D digital chip. The 3D digital chip is a 10 mm^2 high-density reaction plate that has a single array of 20,000 reaction microwells. Each microwell has a diameter of 60 µm and a depth of 500 µm (Figure 1b). The chip was pretreated with a hydrophobic coating on the chip surface to enable the loading and isolation of the LAMP reactions within the microwells. After the addition of the reaction reagent, an oil layer was applied to cover the chip. This step not only facilitates the straightforward isolation of each reaction microwell but also serves as a preventive measure against contamination and reagent evaporation. Following a 45-min incubation at 63°C, microwells containing the target DNA exhibit a green fluorescence signal attributed to successful target amplification, while microwells lacking the target remain devoid of such fluorescence.

Figure 2a shows the schematic of the FQ probe-based LAMP reaction. This assay was developed with the designation of two sets of primers to specifically detect the HPV 16 DNA target. Five LAMP primers (FIP, BIP, F3, B3, and LB) were designed according to the distinct regions of the HPV 16. In the present study, two different types of LBs were constructed: the LB probe is the traditional probe with unlabeled ends. The other probe, named the FQ LB probe, has the same sequence as the LB probe but was tagged with FAM fluorophore at the 5'-end and Iowa Black® RQ quencher at the 3'-end. The quencher functions to inhibit the fluorophore from emitting signals when they are close to

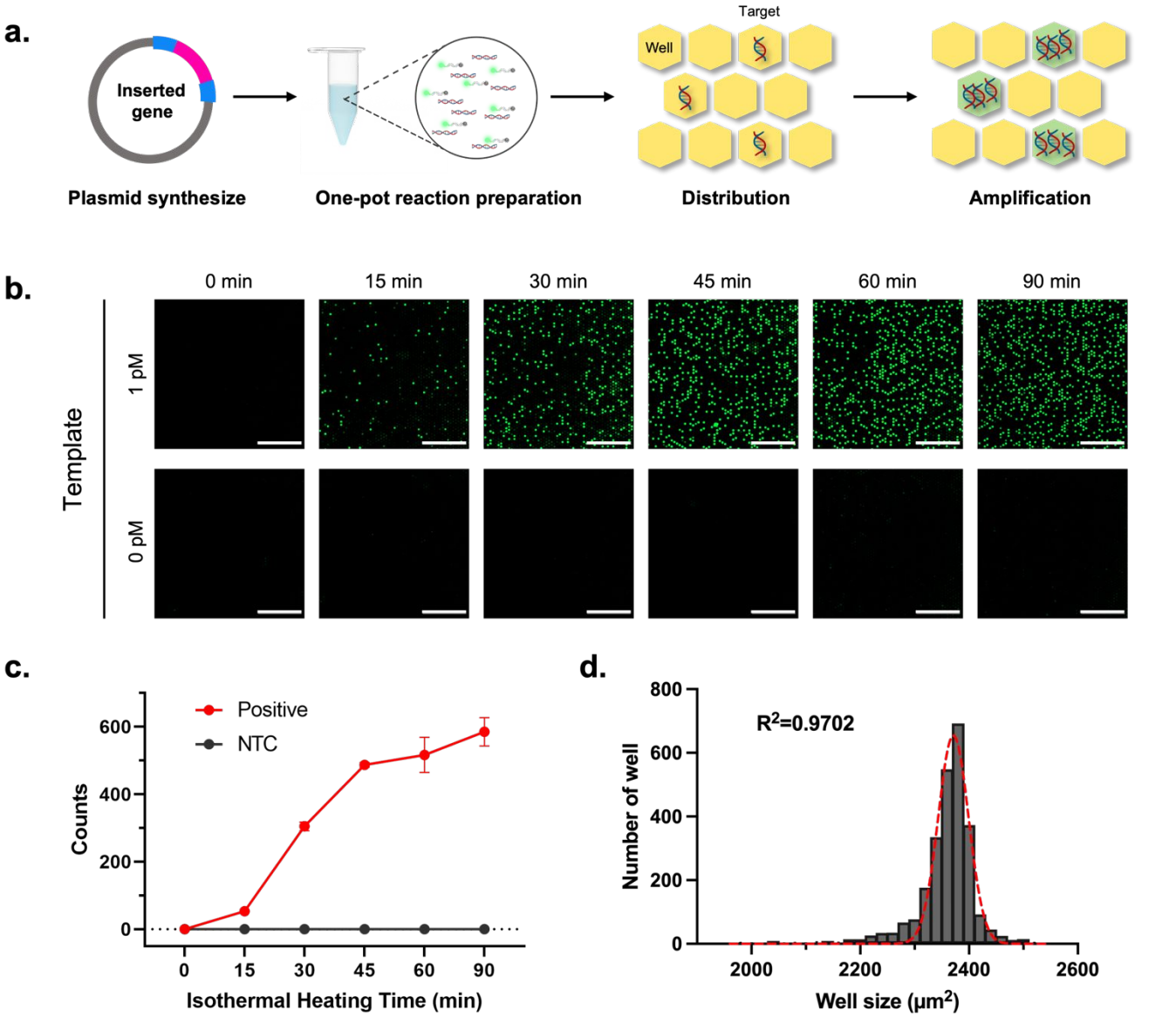

Figure 3 a. The schematic of digital amplification in microwells. b. Endpoint fluorescence micrographs of the digital chip for the HPV 16 detection (1 pM) with various incubation time (0, 15, 30, 45, 60 and 90 min) at 63°C. Scale bar: 1 mm. c. The average positive spots increase to a detectable level within 15 min, and when the time was greater than 45 min, there was no significant change in the positive spots. Error bars denote the standard deviation (n = 5). d. Histogram of well area conforming to Gaussian distribution (R^2=0.9702) at a target concentration of 100 pM, proofing the high uniformity of the reagents in the microwells.

each other. In its unbound state, this probe is quenched and does not emit fluorescence. However, when it binds to a specific complementary target sequence during amplification, DNA polymerase degrades the probe, separating the fluorophore from the quencher. This separation enables the fluorophore to emit a signal, indicating the presence of target. The fluorophore and quencher were placed further from each other to allow them to anneal the stem-loop region of the dumbbell-like LAMP amplicons specifically. As the probe is longer than 20 base pairs, it was designed with an additional internal quencher, that is, an internal quencher /ZEN/ positioned in the middle of the strand. This design was intended to reduce the assay's crosstalk signals, increase the amplification signal, and produce a lower background noise. The concentrations and ratio of the LB and FQ LB primer reactions were optimized, as illustrated in Figure 2b and 2c, the optimal concentration for both LB and FQ LB primer was determined to be 0.4 μM, ensuring efficient amplification and detection. Furthermore, the ideal ratio of LB primers to FQ LB primers was established as 1:1, which optimizes the interaction between the primers and the target sequence. This balance ratio enhances both the sensitivity and specificity of the reaction, leading to more accurate resulting during the amplification process. The fluorescence intensity was measured for the target DNA concentration ranging from 10 aM to 1 pM (Figure 2d), and the positive reaction was clearly observed in the 1 fM sample with both the naked eye and UV illumination. Figure 2e shows the comparison of the fluorescence intensity for positive and negative targets (1 pM), and a clear difference between positive (HPV16) and negative groups (HPV 18 and NTC) is observed.

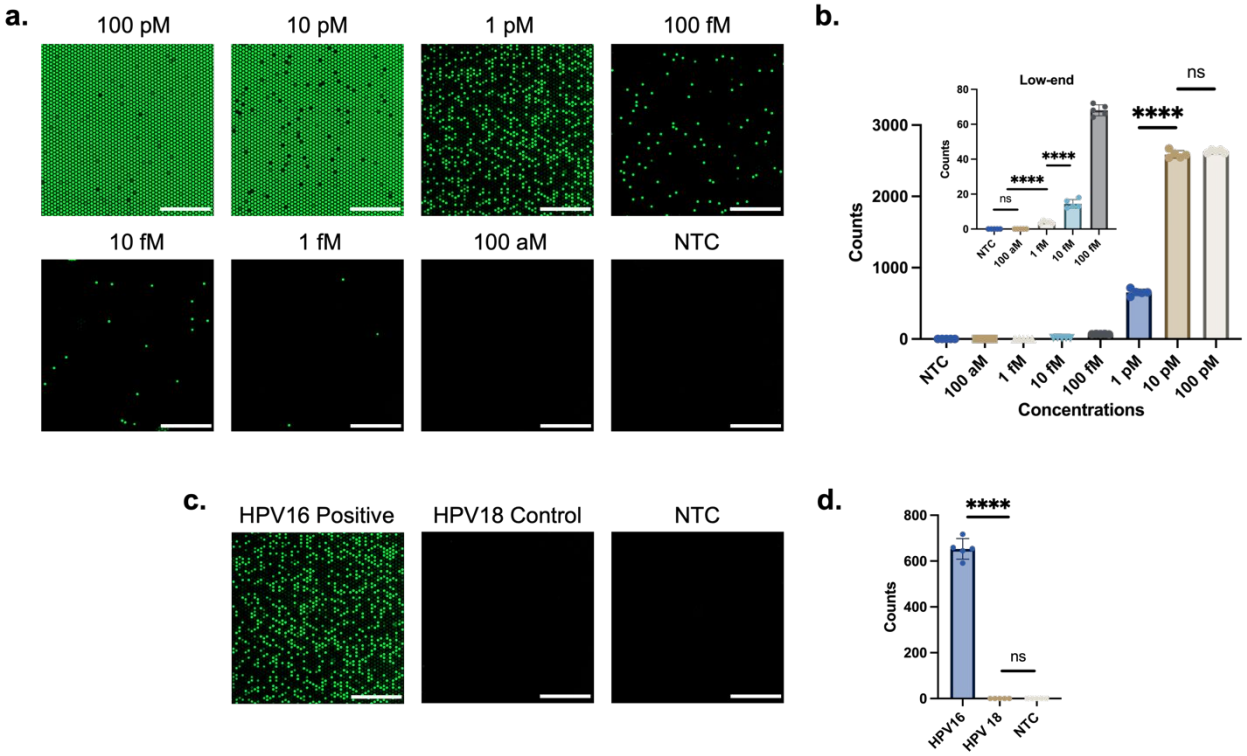

Figure 4 a. End-point fluorescence images of reactions with different starting concentrations of plasmid HPV 16 DNA target within 45 min incubation at 63°C. Scale bar, 1 mm. b. Quantification range of the digital chip. The relationship between positive spots (Y) and concentration of targets (X), from 100 aM to 100 pM. The low-end shows the enlarged view of low concentration range from 100 aM to 100 fM. c. End-point fluorescence images for the specificity of Plasmid HPV 16 PC, Plasmid HPV 18 control, and no template control. Scale bar: 1 mm. d. Detection specificity of the Plasmid HPV 16 DNA target (1 pM) compared with plasmid HPV 18 DNA target (1 pM) and no template control. For each concentration's testing, error bars denote the standard deviation (n = 5). The asterisks represent statistical significance according to a t-test. *P ≤ 0.05, **P ≤ 0.01, ***P ≤ 0.001, ****P ≤ 0.0001.

After optimizing the reaction conditions off-chip, the analytical performance of the microwell chip was investigated. Figure 3a illustrates the typical workflow of the FQ-LAMP assay, encompassing the synthesis of DNA Plasmid which mimics the HPV circular dsDNA genome, preparation of a one-pot LAMP reaction mixture, distribution of the reaction mixture into the chip, and on-chip incubation at 63°C. Figure 3b shows the images of on-chip reactions under a microscope with various incubation times (e.g., 0, 15, 30, 45, 60, and 90 min) using 1 pM HPV plasmid as a target. As shown in Figure 3c, a 45-min incubation is enough for the FQ probe LAMP assay to reach the maximum percentage of the positive spots. The uniformity of the microwell volume was also characterized by ImageJ. As shown in Figure 3d, the average well area was $2371 \pm 28.01\ \mu m^2$ at a target concentration of 100 pM, which conforms to a Gaussian distribution (R^2=0.9702). These results indicate that our chip has high uniformity across all wells and is ideal for digital fluorescence sensing.

By testing various concentrations of HPV 16 DNA plasmid target, the on-chip detection sensitivity was also investigated. As shown in Figure 4a, the digital FQ LAMP assay was performed with a target concentration ranging from 100 aM to 100 pM, and signals can directly be observed by counting the positive spots shown under the microscope. We are able to detect the HPV 16 target with a concentration as low as 1 fM, and the signal is saturated with a concentration greater than 10 pM. The specificity of the digital LAMP assay was also carried out by using similar strains. As shown in Figure 4c, positive spots are observed in the chip loaded with the HPV 16 positive control, whereas not for those negative control samples, such as the HPV 18 control and the no template control, which is consistent with our off-chip results. Additionally, the digital nanofluidic chip provides highly quantitative readouts across target concentrations from 1 fM to 10 pM (Figure 4b), demonstrating an excellent linear relationship (R^2 = 0.9764) between target concentrations (X) and the number of positive spots (Y) (Figure S1), with a dynamic range spanning 5 orders of magnitude. Moreover, notable distinctions exist in the specificity of HPV target detection when compared to other strains (Figure 4d).

The entire pipeline for processing images and classifying the testing samples is shown in Figure 5. To estimate target concentrations from sample images, we first inputted a dataset of training images showcasing results. These images are crucial for creating a baseline for the system's understanding of target appearances at various concentrations. Next, template matching algorithms were applied to detect samples within these images due to the spatial hexagon shape property of each individual sample. We slide this hexagon template across the entire sample image to detect individual samples. The detected samples were sorted based on image intensity levels, ranging from high intensity to low intensity. This sorting is essential to standardizing the analysis across different samples, as the sample image intensity is highly correlated to the target

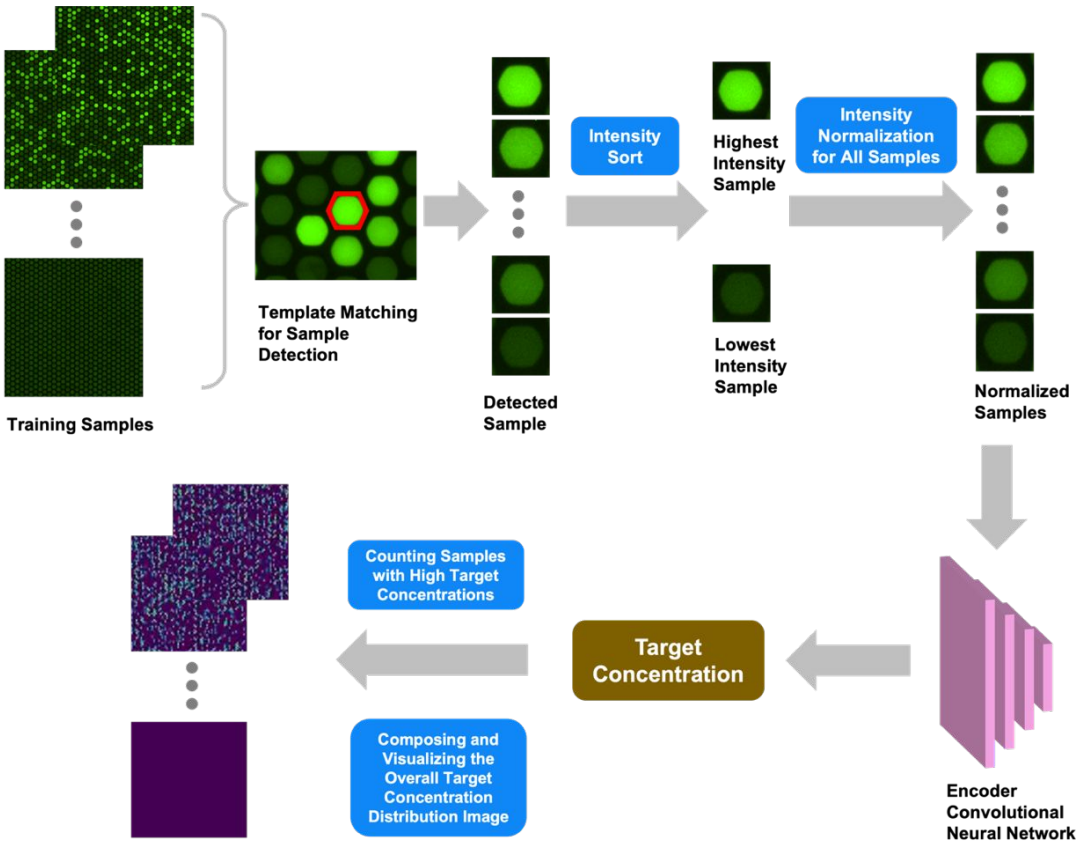

Figure 5 The image processing and testing result classification pipeline for computer vision-enabled HPV target sensing on a Digital Nanofluidic Chip, which involves feature generation, intensity range selection, and feature classification.

concentration. Subsequently, the intensity values of all samples were normalized to account for variations in target concentration. This normalization ensures consistent and reliable data fed into the neural network. Finally, a Convolutional Neural Network (CNN) was trained using these normalized images. The CNN learns the patterns and correlations between the visual characteristics of the target samples and their known concentrations. This learning enables the network to accurately estimate target concentrations in new, unseen images. Eventually, we composed the target concentration result for each individual sample to the entire training sample image with thousands of individual samples and visualized the target concentration distribution. With this learning algorithm, our system can correctly identify all the positive and negative samples, and the network can accurately estimate the target concentration in unseen images.

Discussion

In this study, we developed a novel energy transfer-labeled oligonucleotide probe to create a highly sensitive and specific isothermal amplification assay for nucleic acids detection. We applied it in a digital nanofluidic chip to enable rapid quantitative detection of HPV targets. FQ LB is a single fluorophore and quencher-labeled oligonucleotide probe that can be cleaved by ribonuclease, simultaneously initiating rapid nucleic acid amplification and generating sequence-specific fluorescence. The designed detection method is a process conducted in a closed one-pot system, integrating multi-step reactions within the same enclosed reservoir, thereby mitigating the risk of carryover or cross-contamination arising from post-amplification steps. The quencher restricts the signals by the fluorophore when they are in close proximity. The probes employed in our approach are quenched in the unbound state and emit fluorescence exclusively upon annealing to a specific complementary region during the amplification process, ensuring high sequence specificity. For LB probes shorter than 20 nucleotides, labelling is limited to the ends, while those exceeding 20 nucleotides incorporate an internal quencher at the midpoint, which would otherwise not be quenched due to the length of the DNA strand. This design reduces crosstalk, enhances amplification, and diminishes background noise.[34] In addition, the use of FQ probes does not require a complex pre-processing procedure. Due to the complexity of distinguishing non-specific LAMP amplicons from target amplicons, FQ probes are more specific than conventional LAMP assays using DNA intercalating dyes and can significantly reduce background signals. Therefore, this study reveals the benefits of using FQ LB probes to improve amplicon detection in LAMP assays.

The novel FQ LB probe design not only simplifies the reaction steps but also improves the specificity of the assay. Compared to the commonly used calcein/manganese chloride or SYBR

Table 1. Comparison of representative LAMP-based HPV point-of-care testing methods.

Reaction Principle	Sensing strategy	Labelled material or chemical	Sample-to-result time	Reaction volume	Quantitative or not	Limit of detection per reaction	Reference
LAMP	turbidity	magnesium pyrophosphate	70 min	25 μL	Not	10^4 copies	Ref.[35]
LAMP	fluorescence	EvaGreen dye	30 min	20 μL	Not	5.5×10^4 copies	Ref.[36]
LAMP	colorimetry	gold-nanoparticle	30 min	12.5 μL	Not	10^4 copies	Ref.[37]
LAMP	electrochemical	methylene blue	2 hr	30 μL	Not	1.2×10^4 copies	Ref.[38]
LAMP	electrochemical	antiDIG-HRP	2.5 hr	75 μL	Not	0.1 ng	Ref.[39]
LAMP	digital fluorescence	calcein	110 min	10 μL	Yes	600 copies /μL	Ref.[40]
LAMP	digital fluorescence	fluorescent dye	<45 min	15 μL	Yes	1 fM	This work

green dyes, these traditional choices carry the potential risk of interfering with the reaction components or the detection system and are extremely sensitive to factors such as pH and temperature.[41] Another common detection method is to combine CRISPR with LAMP, however this introduces additional steps and components that increase the complexity of the reaction. This complexity can lead to more errors, thus requiring more extensive optimization and inevitably increasing off-target effects.[42] Our new assay avoids competition between by different substrates minimizing reagent species and can be used for the development of multiplexing LAMP reacttions.[43]

We developed a robust digital amplification system for easy identification of detection targets. This method is a simple patterning method that is unique in its ability to concentrate reagents in a small size. Because the target molecules are assigned to numerous small, separated reaction reservoirs, the positive and negative reservoirs can easily be distinguished from each other without interference. The system is more tolerant to reaction inhibitors, as the potential reaction inhibitors are separated from the reaction mixture, reducing the amplification reaction inhibition in the digital assay and making it well-suited for the detection of low-level targets. We found that due to the multiprobing of the conventional LAMP assays, reactions in Eppendorf tubes are more susceptible to non-specific amplifications due to the cross-linking of amplicons, and aerosols generated during the reaction may cause contamination, leading to false positives.[44] In contrast, no false-positive signals were found in the reaction system of our digital nanofluidic chip. Therefore, digital detection can directly detect nucleic acid in many samples without complicated sample pre-treatment and nucleic acid purification processes.

Our microliter digital microwells enable the quantitative detection of nucleic acids without the need for calibration curves, thereby improving the accuracy of detecting low-copy nucleic acid templates. Conventional tube-based reactions, such as colorimetric,[45] fluorescence detection,[46] and turbidity-based assays,[35] pose challenges for accurate quantitative detection. Therefore, they are more appropriate for qualitative assessments, primarily serving to differentiate between positive and negative results without offering precise concentration measurements. In contrast, the nano digital chip enables straightforward and highly accurate quantitative detection, as it facilitates individual target molecule counting, which translates into precise measurements of target concentrations. This feature makes digital chip technology highly effective for applications requiring detailed quantification over a broad dynamic range. Table 1 presents a comparison of representative LAMP-based HPV point-of-care testing methods. The ability to quantitatively detect nucleic acids without relying on calibration curves is a key feature that enhances accuracy, particularly in low-copy nucleic acid template detection. In addition, compared to droplet microfluidic chips that produce monodisperse droplets, fixed-structure chambers are more stable and suitable for real-time monitoring.[47] The compartmentalization of nucleic acid in digital detection enables individual amplification and detection, enhancing sensitivity to the single-molecule level. This surpasses the sensitivity achievable with traditional isothermal amplification reactions, which often require intricate primer screening and probe optimization.

We have developed a computer vision-based data analysis system. Through this learning process, our system correctly identifies both positive and negative samples, and the network can also accurately estimate the concentration of targets in

unseen images. In the end, the classification accuracy of separating detected positive samples from negative samples is 100%. Our method integrates both deep learning and classical computer vision techniques to achieve optimal outcomes. Classical computer vision methods are computationally efficient and well-suited for sample detection. After sorting the samples based on intensity values, they can be evaluated in a standardized range in later deep learning stage. This approach makes our method a robust and powerful tool for analysing target concentrations, with important applications in areas such as molecular detection and clinical diagnosis. The application of computer vision in biosensors has great prospects, as it enables large-scale, automated, high-throughput, and multi-target detection compared with the traditional analysis methods.[48] The prospect of enhancing sensitivity, specificity, and efficiency in biosensing through computer vision signifies a significant leap forward in the realm of diagnostic and analytical methodologies. It stands as a vital tool for the future development of traditional biosensors toward intelligent biosensors.[49]

Human papillomaviruses (HPVs) are associated with a variety of malignancies, of which cervical cancer is the most important and prevalent. There are many HPV types; HPV 16/18 are the most carcinogenic. The HPV tests that are currently most widely applied are based on two principles. The first, as used in the HCII assay, the analytical sensitivity of the HCII assay is at the picogram level of HPV DNA. Another method is PCR assays which can reach the sub-picogram level.[50] A quantitative assay might be more effective in identifying women at risk of progression, thus improving both negative and positive predictive values.[51] Our innovative detection approach represents a major improvement. Not only does it surpass the previously established femtomolar detection limit, but it also offers the added advantage of enabling precise quantification, particularly crucial when dealing with samples containing lower concentrations of HPV DNA. In clinical settings, viral load is typically measured in copies per 10^3 cells. We also observed that when the clinically relevant HPV16 viral load exceeds 22,000 copies per 10^3 cells, women with prevalent high-grade lesions can be identified.[52] A Pap smear slide should have at least 5,000 squamous epithelial cells to be considered adequate.[53] In our study, we demonstrated that the detection limit for a 2 µL input target was 1 fM (600 copies/µL), offering a dynamic range across five orders of magnitude, making it applicable for future cancer staging diagnostics. This heightened sensitivity and quantification capability promise to revolutionize HPV screening protocols, ultimately leading to more effective early detection and prevention of HPV-related malignancies, particularly cervical cancer. Recent research demonstrates that cervical cells can be simply prepared by suspending them in normal saline oral rinses and then boiling at 100 °C for 5 min, followed by LAMP-based detection for HPV target.[54] In the future, we plan to apply our nano digital chip to assess patient samples across different stages of cervical lesions.

Experimental

Materials and reagents:

Deoxynucleotide (dNTP) solution mix (10 mM of each), Bst 2.0 WarmStart DNA polymerase (8 U/µL), $MgSO_4$ (100 mM), 10 × Isothermal Amplification Buffer (200 mM Tris–HCl, 500 mM KCl, 100 mM $(NH_4)_2SO_4$, and 20 mM $MgSO_4$, 1.0% Tween 20 and pH 8.8 at 25 °C) were purchased from New England BioLabs (Ipswich, MA). Primers, FQ probe, and the plasmid pCDNA3.1(+) containing 450-bp HPV 16 and HPV 18 gene sequences were purchased from either Integrated DNA Technologies (Coralville, IA) or synthesized by Genscript. All the sequence information of the primers and target sequences is listed in Table S1. The primer sequences were designed according to the LAMP Primer Design Tool from the New England BioLabs website. The QuantStudio 3D digital 20K chip kit (Version 2) was purchased from Thermo Fisher Scientific (Waltham, MA).

Preparation of the target plasmids:

The 450-base pair (bp) target sequences of the HPV-L1 gene from HPV16 and HPV18 were synthesized by GenScript (GenScript USA, Inc, Piscataway, NJ, USA) with HindIII and NotI restriction enzyme sites flanking the sequence. These restriction sites were incorporated to facilitate subsequent cloning steps. The synthesized gene was designed to yield a 463-bp product that was then inserted into the cDNA3.1(+) expression vector to yield a 5,820 bp plasmid. The insert sequence was verified post-synthesis through sequencing analysis (QuintaraBio, Frederick, MD, USA).

Off-chip isothermal amplification assay:

We performed all the HPV 16 target detection with FQ LB (fluorescence quenched) probe-based LAMP assay. Briefly, 25 µl of the reaction for each experiment contained 2.5 µl of 10x Isothermal Amplification Buffer, 1.5 µL of MgSO4 (100 mM), 3.5 µL dNTP mix (10 mM), 2.5 µL of 10x target-specific primer mix (FIP/BIP 16 µM, F3/B3 2 µM, LoopB 4 µM, FQ LB probe 4 µM), 1 µL of Bst 2.0 WarmStart DNA Polymerase (8 U/µL), and 2 µL of HPV target with different concentrations. The rest of the reaction contained 12 µL of nuclease-free water. The LAMP conditions were optimized for the reaction with a mixture of LB/FQ LB primers at concentrations of 0.2, 0.4, and 0.6 µM, respectively. We also optimized the ratio of LB/FQ LB primers with 2:1, 2:2, and 2:4, respectively. The reaction was incubated at 63°C for 45 min. After incubation, the tubes were placed under a Maestrogen UltraSlim LED blue light illuminator (Pittsburgh, PA) to take images (Canon EOS 6D, Canon, Japan). The endpoint fluorescence was measured by a plate reader (BioTek Cytation 5, Agilent, CA, USA).

On-chip isothermal digital amplification assay:

The digital nanofluidic chip is a 10 mm^2 high-density reaction plate that has a single array of 20,000 reaction microwells with 15 µL volume for each well. The 15 µL reaction mixture contained 1.5 µL of 10x Isothermal Amplification Buffer, 0.9 µL of $MgSO_4$ (100 mM), 2.1 µL dNTP mix (10 mM), 1.5 µL of 10x

target-specific primer mix (FIP/BIP 16 µM, F3/B3 2 µM, LoopB 4 µM, FQ LB probe 4 µM), 0.6 µL of Bst 2.0 WarmStart DNA Polymerase (8000 U/mL), 1.2 µL of target DNA, and 7.2 µL of nuclease-free water. After assay mixing, the 15 µL reaction mixture was loaded into the chip, and mineral oil was used to seal the loading port. The device was placed on a heat block and incubated at 63°C for 45 min.

Data acquisition and analysis:

After incubation, the chip was quantified using a BioTek Cytation 5 Cell Imaging Multimode Reader (Agilent, CA, USA) with a 4x magnification objective. Every image was captured in ~30 s of laser irradiation, and the irradiation was turned off until the next imaging. Five distinct regions (3.5 x 3.5 mm) without overlapping areas were randomly captured by microscopy to cover approximately 2,750 microwells. The number of positive spots and corresponding fluorescence intensity were measured by using the ImageJ software (bit depth: 8 bits; 1,992 x 1,992 pixels). GraphPad Software Prism 9.5.1 was used to plot real-time fluorescence curves, analyse linear regression, and verify statistical significance between different assay groups.

Conclusions

In summary, our study presents a comprehensive approach to nucleic acid detection, utilizing an innovative energy transfer-labeled oligonucleotide probe in tandem with a digital nanofluidic chip and advanced data analysis technique. The incorporation of FQ LB probes offers advantages like enhanced specificity, reduced background noise, and simplified processing, while the closed one-pot procedure minimizes the risk of contamination. Our robust digital amplification system enables rapid and quantitative detection of nucleic acid targets, even at low concentrations, facilitated by microliter digital microwells that enhance sensitivity and enable easy quantitative analysis without calibration curves.

Additionally, integration of a computer vision-based data analysis system improves target identification and concentration estimation, promising large-scale, automated, and high-throughput molecular detection applications. Together, these innovations signify significant advancements in sensitivity, specificity, and efficiency, holding promise for the development of intelligent biosensors and transforming molecular detection in clinical diagnosis and beyond.

Conflicts of interest

There are no conflicts to declare.

Acknowledgements

This work was supported by NIH R35GM 142763, NIH 75N93023C00056-0-9999-1, and USDA NIFA 2022-67021-41478.

Notes and references

1 Cervical cancer, https://www.who.int/health-topics/cervical-cancer, (accessed January 28, 2024).
2 Human Papillomavirus (HPV), https://www.who.int/teams/health-product-policy-and-standards/standards-and-specifications/vaccine-standardization/human-papillomavirus, (accessed January 24, 2024).
3 M. Arbyn, M. Simon, E. Peeters, L. Xu, C. J. L. M. Meijer, J. Berkhof, K. Cuschieri, J. Bonde, A. Ostrbenk Vanlencak, F.-H. Zhao, R. Rezhake, M. Gultekin, J. Dillner, S. de Sanjosé, K. Canfell, P. Hillemanns, M. Almonte, N. Wentzensen and M. Poljak, *Clin Microbiol Infect*, 2021, **27**, 1083–1095.
4 J. Wang, K. M. Elfström, C. Lagheden, C. Eklund, K. Sundström, P. Sparén and J. Dillner, *PLOS Medicine*, 2023, **20**, e1004304.
5 Y. Zhao, F. Chen, Q. Li, L. Wang and C. Fan, *Chem. Rev.*, 2015, **115**, 12491–12545.
6 C. Yan, J. Cui, L. Huang, B. Du, L. Chen, G. Xue, S. Li, W. Zhang, L. Zhao, Y. Sun, H. Yao, N. Li, H. Zhao, Y. Feng, S. Liu, Q. Zhang, D. Liu and J. Yuan, *Clinical Microbiology and Infection*, 2020, **26**, 773–779.
7 T. Notomi, Y. Mori, N. Tomita and H. Kanda, *J Microbiol.*, 2015, **53**, 1–5.
8 L. Becherer, N. Borst, M. Bakheit, S. Frischmann, R. Zengerle and F. von Stetten, *Anal. Methods*, 2020, **12**, 717–746.
9 I. M. Lobato and C. K. O'Sullivan, *TrAC Trends in Analytical Chemistry*, 2018, **98**, 19–35.
10 R. Peng, X. Chen, F. Xu, R. Hailstone, Y. Men and K. Du, *Nanoscale Horizons*, 2023, **8**, 1677–1685.
11 M. Bao, S. Zhang, C. ten Pas, S. J. Dollery, R. V. Bushnell, F. N. U. Yuqing, R. Liu, G. Lu, G. J. Tobin and K. Du, *Lab on a Chip*, 2022, **22**, 4849–4859.
12 L. Gu, W. Yan, L. Liu, S. Wang, X. Zhang and M. Lyu, *Pharmaceuticals*, 2018, **11**, 35.
13 M. M. Ali, F. Li, Z. Zhang, K. Zhang, D.-K. Kang, J. A. Ankrum, X. C. Le and W. Zhao, *Chem. Soc. Rev.*, 2014, **43**, 3324–3341.
14 R. Wang, X. Zhao, X. Chen, X. Qiu, G. Qing, H. Zhang, L. Zhang, X. Hu, Z. He, D. Zhong, Y. Wang and Y. Luo, *Anal. Chem.*, 2020, **92**, 2176–2185.
15 B. Deiman, P. van Aarle and P. Sillekens, *Mol Biotechnol*, 2002, **20**, 163–179.
16 N. Cook, *Journal of Microbiological Methods*, 2003, **53**, 165–174.
17 R. Asadi and H. Mollasalehi, *Analytical Biochemistry*, 2021, **631**, 114260.
18 W. Liu and Y. Zhu, *Analytica Chimica Acta*, 2020, **1113**, 66–84.
19 D. M. Cate, J. A. Adkins, J. Mettakoonpitak and C. S. Henry, *Anal. Chem.*, 2015, **87**, 19–41.
20 N. Van Thanh Nguyen, M. Taverna, C. Smadja and T. D. Mai, *The Chemical Record*, 2021, **21**, 149–161.
21 M. Song, L. Feng, P. Huo, M. Liu, C. Huang, F. Yan, Y. Lu and T. Xu, *Nat. Nanotechnol.*, 2023, **18**, 71–78.
22 A. Stollmann, J. Garcia-Guirado, J.-S. Hong, P. Rüedi, H. Im, H. Lee, J. Ortega Arroyo and R. Quidant, *Nat Commun*, 2024, **15**, 4109.
23 M. Parida, S. Sannarangaiah, P. K. Dash, P. V. L. Rao and K. Morita, *Reviews in Medical Virology*, 2008, **18**, 407–421.
24 L. Niessen, J. Luo, C. Denschlag and R. F. Vogel, *Food Microbiology*, 2013, **36**, 191–206.

25 M. Soroka, B. Wasowicz and A. Rymaszewska, *Cells*, 2021, **10**, 1931.
26 T. L. Quyen, T. A. Ngo, D. D. Bang, M. Madsen and A. Wolff, *Frontiers in Microbiology*.
27 K. Nath, J. W. Sarosy, J. Hahn and C. J. Di Como, *Journal of Biochemical and Biophysical Methods*, 2000, **42**, 15–29.
28 H. Bai, Y. Liu, L. Gao, T. Wang, X. Zhang, J. Hu, L. Ding, Y. Zhang, Q. Wang, L. Wang, J. Li, Z. Zhang, Y. Wang, C. Shen, B. Ying, X. Niu and W. Hu, *Biosensors and Bioelectronics*, 2024, **248**, 115968.
29 Y. Cao, C. Ye, C. Zhang, G. Zhang, H. Hu, Z. Zhang, H. Fang, J. Zheng and H. Liu, *Food Control*, 2022, **134**, 108694.
30 W. Yin, J. Zhuang, J. Li, L. Xia, K. Hu, J. Yin and Y. Mu, *Small*, 2023, **19**, 2303398.
31 B. Coelho, B. Veigas, E. Fortunato, R. Martins, H. Águas, R. Igreja and P. V. Baptista, *Sensors*, 2017, **17**, 1495.
32 Z. Yu, L. Xu, W. Lyu and F. Shen, *Lab on a Chip*, 2022, **22**, 2954–2961.
33 F. X. Liu, J. Q. Cui, H. Park, K. W. Chan, T. Leung, B. Z. Tang and S. Yao, *Anal. Chem.*, 2022, **94**, 5883–5892.
34 J. M. Wong Tzeling, E. A. R. Engku Nur Syafirah, A. A. Irekeola, W. Yusof, N. N. Aminuddin Baki, A. Zueter, A. Harun and Y. Y. Chan, *Analytica Chimica Acta*, 2021, **1171**, 338682.
35 C. Saetiew, T. Limpaiboon, P. Jearanaikoon, S. Daduang, C. Pientong, A. Kerdsin and J. Daduang, *Journal of Virological Methods*, 2011, **178**, 22–30.
36 F. Sun, A. Ganguli, J. Nguyen, R. Brisbin, K. Shanmugam, D. L. Hirschberg, M. B. Wheeler, R. Bashir, D. M. Nash and B. T. Cunningham, *Lab on a Chip*, 2020, **20**, 1621–1627.
37 N. M. Rodriguez, W. S. Wong, L. Liu, R. Dewar and C. M. Klapperich, *Lab Chip*, 2016, **16**, 753–763.
38 M. Zamani, J. M. Robson, A. Fan, M. S. Jr. Bono, A. L. Furst and C. M. Klapperich, *ACS Cent. Sci.*, 2021, **7**, 963–972.
39 M. Bartosik, L. Jirakova, M. Anton, B. Vojtesek and R. Hrstka, *Analytica Chimica Acta*, 2018, **1042**, 37–43.
40 T. D. Rane, L. Chen, H. C. Zec and T.-H. Wang, *Lab on a Chip*, 2015, **15**, 776–782.
41 D. Das, C.-W. Lin and H.-S. Chuang, *Biosensors*, 2022, **12**, 1068.
42 X. Ding, K. Yin, Z. Li, M. M. Sfeir and C. Liu, *Biosensors and Bioelectronics*, 2021, **184**, 113218.
43 A. Bektaş, *Food Anal. Methods*, 2018, **11**, 686–692.
44 K. Karthik, R. Rathore, P. Thomas, T. R. Arun, K. N. Viswas, K. Dhama and R. K. Agarwal, *MethodsX*, 2014, **1**, 137–143.
45 W. E. Huang, B. Lim, C.-C. Hsu, D. Xiong, W. Wu, Y. Yu, H. Jia, Y. Wang, Y. Zeng, M. Ji, H. Chang, X. Zhang, H. Wang and Z. Cui, *Microbial Biotechnology*, 2020, **13**, 950–961.
46 Z. Fan, X. Feng, W. Zhang, N. Li, X. Zhang and J.-M. Lin, *Talanta*, 2020, **217**, 121015.
47 S.-Y. Teh, R. Lin, L.-H. Hung and A. P. Lee, *Lab on a Chip*, 2008, **8**, 198–220.
48 R. Antiochia, *Biosensors and Bioelectronics*, 2021, **173**, 112777.
49 L. Liu and K. Du, *Biomicrofluidics*, 2024, **18**, 011301.
50 P. J. Snijders, A. J. van den Brule and C. J. Meijer, *The Journal of Pathology*, 2003, **201**, 1–6.
51 A. Molijn, B. Kleter, W. Quint and L.-J. van Doorn, *Journal of Clinical Virology*, 2005, **32**, 43–51.
52 M. Saunier, S. Monnier-Benoit, F. Mauny, V. Dalstein, J. Briolat, D. Riethmuller, B. Kantelip, E. Schwarz, C. Mougin and J.-L. Prétet, *Journal of Clinical Microbiology*, 2008, **46**, 3678–3685.
53 H. C. Kitchener, M. Gittins, M. Desai, J. H. Smith, G. Cook, C. Roberts, L. Turnbull, H. C. Kitchener, M. Gittins, M. Desai, J. H. Smith, G. Cook, C. Roberts and L. Turnbull, *A study of cellular counting to determine minimum thresholds for adequacy for liquid-based cervical cytology using a survey and counting protocol*, NIHR Journals Library, 2015.
54 D. T. Vo and M. D. Story, *Molecular and Cellular Probes*, 2021, **59**, 101760.

Data for this article are available at UC-Riverside Google Driver system.